PROCEEDINGS of ISMA 2019
International Symposium on Music Acoustics

13 - 17 September 2019 in Detmold, Germany

# Finite element simulation of radiation impedances with applications for musical instrument design

Péter RUCZ[(1)], Judit ANGSTER[(2)], András MIKLÓS[(2)]

[(1)]Budapest University of Technology and Economics, Hungary, rucz@hit.bme.hu
[(2)]Fraunhofer Institute for Building Physics, Germany

**Abstract**

Creating a musical instrument often involves designing acoustical resonators. The natural frequency and the quality factor of the resonator are affected by the radiation impedance to a significant extent. Therefore attaining as much a priori knowledge as possible on the radiation characteristics is desirable. On the other hand, for the sake of efficiency, radiation characteristics are most often reduced to a sole frequency dependent radiation impedance function. A finite element approach for the calculation of self and mutual radiation impedances was introduced recently [Rucz, JASA 143(4) 2449–2459], which is suitable for these purposes.

In this contribution, the methodology is applied and extended with different applications in musical instrument design. In particular, the radiation from the mouth regions of organ pipes and recorders are examined. The geometrical parameters having the most significant effect on the radiation characteristics are analyzed and the results are compared to previously published data. As another example, finite element simulations of Helmholtz resonators of a mallet percussion instrument are introduced. In this case, the length correction effect of the sound bars partially covering the opening of the resonators is studied. Finally, the effect of viscous losses on the quality of the natural resonance is investigated.

Keywords: Radiation impedance, finite element method, resonator design

## 1 INTRODUCTION

Designing the resonator of a musical instrument can involve various challenges, one of them being the characterization of the acoustical radiation from the openings into the exterior sound field. The coupling between the interior and exterior acoustical fields affects the natural frequency and the quality factor of the resonator and also the radiation directivity of the instrument. Therefore the accurate prediction of the radiation characteristics of resonators is desirable for the efficient design of musical instruments. However, the acoustical radiation problem can only be solved analytically in case of very simple geometries, and numerical approximations must be used to handle more complex geometrical arrangements.

Numerical simulations can provide a wealth of information and they allow for handling almost arbitrarily complex geometries. On the other hand, they are computationally involving, which renders their usefulness strictly limited in applications such as real time sound synthesis or parameter optimization. Thus, for the sake of computational efficiency, it is useful to reduce the radiation characteristics into a sole frequency dependent radiation impedance function by post-processing the results of 3D field simulations.

In this paper the finite element method is utilized together with a post-processing technique relying on plane wave decomposition in order to attain the frequency dependent radiation impedance in various geometrical configurations. The extracted radiation impedance function can then be used in a simplified waveguide or concentrated parameter model of the resonator. Such “hybrid” models preserve the accurate representation of the geometry and hence the radiation characteristics, while they enable rapid calculations.

In this contribution two different applications are studied. After introducing the methodology briefly, the mouth impedance of recorders and organ pipes are examined with different geometrical parameters. Then, the design of Helmholtz resonators for a mallet percussion instrument is investigated with taking the effect of the sound bars on the radiation properties into account. Finally, the paper is concluded by a short summary.

## 2 METHODOLOGY

Simulation of radiation impedances involving complex geometries is performed in this paper based on the finite element method (FEM) following the approach proposed by Rucz [1]. As radiation problems are examined here, infinite computational domains need to be emulated in the FEM. For this purpose the infinite element approach is utilized, i.e., a truncated domain is meshed using standard finite elements and the infinite elements are attached to the truncated boundary. By means of discretization, the Helmholtz equation is transformed into a matrix equation of the form

$$\left(\mathbf{K}+\mathrm{j}\omega\mathbf{C}-\omega^2\mathbf{M}\right)\mathbf{p}=-\mathrm{j}\omega\mathbf{A}\mathbf{v}, \tag{1}$$

where the matrices **K**, **C**, and **M** are the stiffness, damping, and mass matrices, respectively, **A** is the boundary mass matrix, and the vectors **p** and **v** contain the weights of the pressure and normal particle velocity. The angular frequency is $\omega$ and the imaginary unit is denoted by j. With the proper boundary conditions, the solution of (1) is unique and the sound pressure field in the whole domain is represented by the weights **p** and the corresponding shape functions.

To be able to utilize the results of the finite element simulation in a simplified waveguide or concentrated parameter model, it is necessary to post-process the simulated field and express "lumped" parameters. In particular, the frequency dependent radiation impedance is of primary interest in case of resonator design. In the following, radiation from a straight tube with an irregular opening (such as a tone hole, or the mouth of a flue instrument) is considered. Far from the opening and under the cut-on frequency of transverse modes of the duct the pressure field is essentially one-dimensional and can be written as the d'Alembert solution

$$p(z)=p^{+}\mathrm{e}^{-\mathrm{j}kz}+p^{-}\mathrm{e}^{+\mathrm{j}kz}. \tag{2}$$

where $p^{+}$ and $p^{-}$ are complex amplitudes, $z$ denotes the distance from the opening along the duct, and $k=\omega/c$ is the wave number with $c$ representing the speed of sound.

The complex amplitudes $p^{+}$ and $p^{-}$ in (2) are found by fitting the two exponential functions to the simulated sound pressure field. This is done by choosing a number of virtual microphone locations along the axis of the tube and solving an overdetermined set of equations. Finally, the frequency dependent reflection coefficient $R$, and the radiation impedance $Z$ are obtained using the relation

$$\frac{p^{-}}{p^{+}}=R=-|R|\,\mathrm{e}^{-2\mathrm{j}k\Delta L}=\frac{Z-Z_0}{Z+Z_0}, \tag{3}$$

with $Z_0$ denoting the plane wave impedance. The third expression of (3) contains the frequency dependent length correction (or end correction) $\Delta L$ that is the primary quantity examined in this paper. The length correction is directly related to the change of natural frequencies resulting from the opening.

In [1] it was shown that the theory can be extended to treat multiple coupled ducts and Salmon horns as well. Furthermore, it was also found that the resulting error of fitting the decomposition (2) to the pressure field serves as a good indicator of the reliablility of the evaluated impedance. In this paper only the straight duct formulation is used for simulating radiation impedances of different geometries.

## 3 WINDOW IMPEDANCES OF FLUE INSTRUMENTS

Flue instruments produce sound by means of an oscillating air jet forming at the mouth opening of the resonator. The mouth of a recorder or an organ pipe is a rectangular or nearly rectangular opening on the pipe. The radiation impedance of this opening has a great effect on the natural frequencies of the resonator and hence its accurate prediction is important for a proper resonator design. However, the geometry of the mouth opening is fairly complex, making the estimation of the radiation impedance a non-trivial task.

The window impedance and length correction of flue instruments have already been studied in a number of contributions. Without aiming at completeness a few of these examinations are summarized here briefly. The

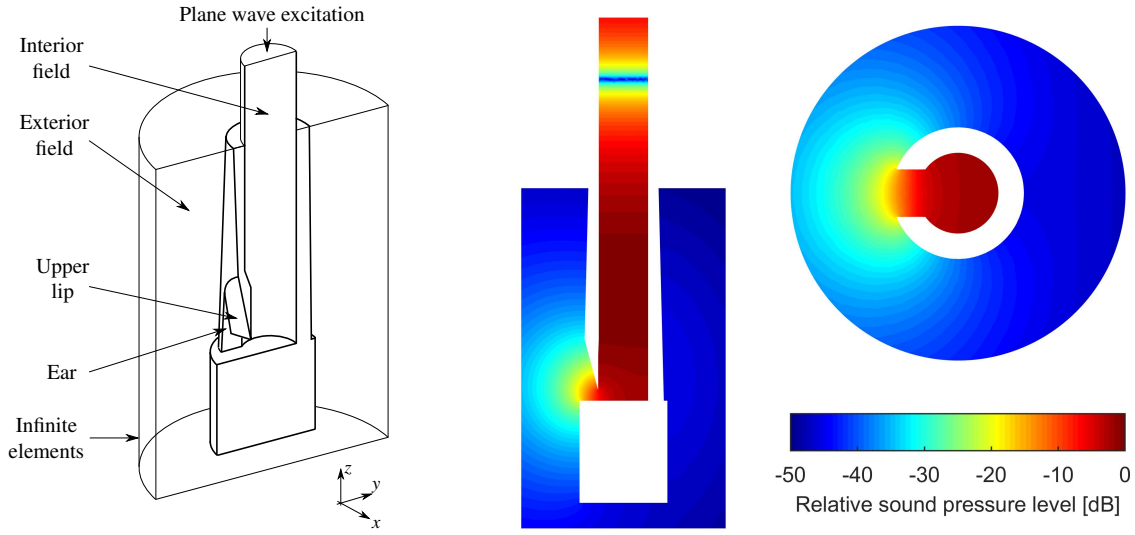


(a) Simulation arrangement

(b) Radiation from the mouth of the alto recorder at $f = 1\,\mathrm{kHz}$

Figure 1. Finite element simulation of the sound radiation from the mouth of a recorder

mouth correction of organ pipes was studied by Ingerslev & Frobenius [2] and an approximate model for the correction was proposed. The window length of different recorders was examined and compared to a theoretical model taking the effect of ears into account by Lyons [3]. Based on somewhat different considerations, the window impedance of a recorder-like instrument was also investigated by Verge *et al.* [4]. In the latter study the length correction of the mouth was assumed to consist of three parts representing the effect of the constriction, the ears, and the radiation into free field, respectively. The model of Verge *et al.* was recently extended by Ernoult & Fabre [5] who simulated the window impedance of recorders using the FEM with simplified geometries. Their model is able to take the effect of the edge angle and ears into account. In this paper geometrically more realistic finite element models are considered and the simulated window length corrections of recorders and organ pipes with different geometries are compared to that of previous studies.

Figure 1(a) shows the arrangement of the finite element simulation, illustrating the geometry of the longitudinal section of the head of a recorder. The main bore is driven by plane wave excitation and radiates into the exterior field through the mouth opening. The upper lip has a sharp edge of angle $\alpha$ at its bottom and it is surrounded by the ears on both sides. The wind channel and the upstream section of the flute head are replaced by a solid cylinder. A cylindrical region of the exterior area is also meshed by finite elements and the infinite elements emulating free field radiation conditions are attached to the outer surface of this cylinder. Similar arrangements were created for simulating the mouth regions of a rectangular and a circular flue organ pipe. The latter pipe does not have ears and the thickness of its walls is much smaller than that of other models. All meshes were generated using the parametric finite element mesh generation tool Gmsh [6]. Figure 1(b) displays the simulated pressure field along the longitudinal section of the bore and the cross section of the mouth of the alto recorder at $f = 1\,\mathrm{kHz}$. The standing waves due to reflections from the mouth are clearly visible inside the bore. The near-field directivity of the opening is also observable both in the horizontal and vertical planes.

Various configurations were simulated using the FEM and the proposed post-processing technique. Figure 2 summarizes the results of the investigation. In Figure 2(a) the window length corrections of different recorders are compared to each other. The dimensions of the recorders were chosen as given in [5]. The frequency dependence of the length correction is not examined in [5], but the low frequency values of the simulated corrections are in good agreement with those of the aforementioned paper. The alto recorder examined by

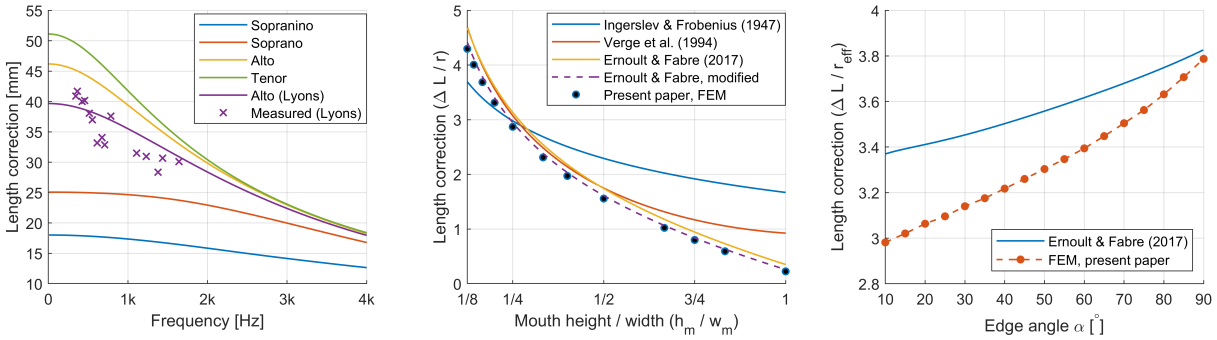


(a) Window corrections of recorders (b) Effect of mouth shape (c) Effect of edge angle

Figure 2. Simulation results of the length corrections of recorders and organ pipes compared to various models

Lyons [3] has a bit different dimensions. The length corrections evaluated from the played frequencies in [3] are also marked on the diagram showing and a fairly good correspondence with the simulation results. It is also observed that the frequency dependence of the correction is significant in the musical range of the instrument.

The low frequency length corrections of a cylindrical thin-walled flue organ pipe with different mouth geometries are shown in Figure 2(b). The simulations were run with changing the height of the mouth opening $h_\mathrm{m}$ while keeping the width of the mouth constant as $w_\mathrm{m} = \pi r/2$, with $r$ denoting the inner radius of the pipe. The finite element results are compared to predictions of different models. Ingerslev & Frobenius [2] substitute the mouth opening with an equivalent ellipse having the same area and height to width ratio as the pipe mouth. This approximation shows a good agreement with the simulation results in the region where $h_\mathrm{m}/w_\mathrm{m} \approx 1/4$, a ratio often applied in organ building practice. Farther away from this ratio the deviations between the prediction and simulation become large. The model of Verge *et al.* [4] that estimates the correction as the sum effect of a constriction and radiation into free space gives a good fit to the simulation results if $h_\mathrm{m}/w_\mathrm{m} < 1$. An even better estimation is obtained by the model of Ernoult & Fabre [5] that is based on a function fitted to finite element simulation results. The best agreement is attained if their radiation correction $l_r = 0.695 r_\mathrm{m}$, with $r_\mathrm{m} = \sqrt{h_\mathrm{m} w_\mathrm{m}/\pi}$ denoting the effective radius of the mouth, is replaced by the theoretical value of an unflanged pipe $l_r = 0.613 r_\mathrm{m}$. The re-calculated corrections are shown as "Ernoult & Fabre, modified" in the diagram. The deviations between this model and the simulations are $< 3\%$ in all cases. This modification seems rational, as the thickness of the walls surrounding the mouth is much smaller than that of the recorder models of [5].

In the third study, the effect of the angle of the edge on the low frequency length correction is investigated in case of a rectangular wooden pipe. The pipe has a square cross section with 80 mm width and depth and the height of the mouth is chosen as $h_\mathrm{m} = 20$ mm. The walls forming the ears at the side of the pipe mouth have a thickness of 15 mm. The angle of the edge is varied between $10° \leq \alpha \leq 90°$ in $5°$ steps in the simulations. To our knowledge, the effect of the edge angle is only taken into account in the model of Ernoult & Fabre [5], thus the simulation results are compared to this model in Figure 2(c). Only the low frequency correction is plotted, normalized by the effective radius of the pipe $r_\mathrm{eff}$. While a good agreement is found at large angles $\alpha \approx 90°$ a deviation of $\approx 10\%$ is observed for small angles $\alpha \approx 10°$. The discrepancies may stem from the somewhat different geometrical arrangements used in the two studies or the data fit formula applied in [5].

## 4 RESONATOR DESIGN OF A MALLET PERCUSSION INSTRUMENT

In this section the design of an Orff instrument is examined. The mallet percussion instrument at hand has thirteen sound bars made of rosewood and arranged in the diatonic scale from C4 (262 Hz) to A5 (880 Hz). The first few longitudinal bending modes of the sound bars are tuned by cutting the typical arch profile into

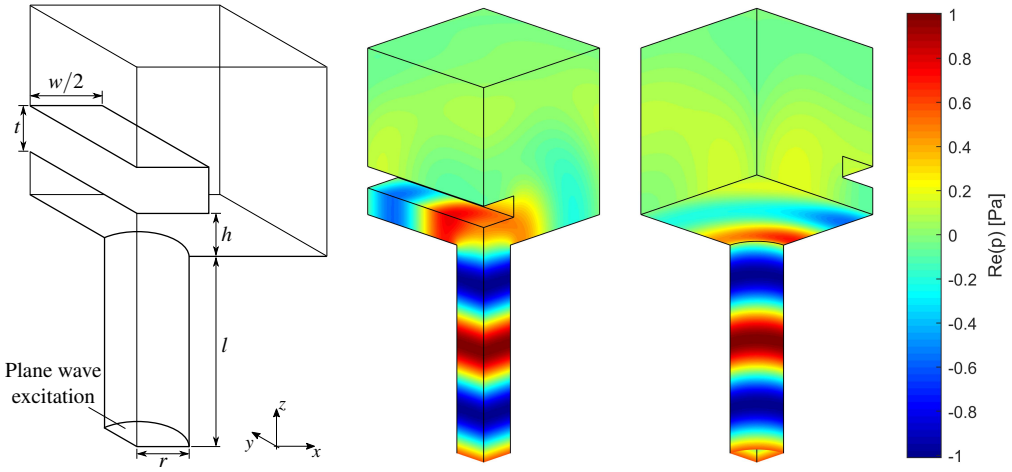


(a) Arrangement and main parameters (b) Finite element simulation result at $kr = 1.72$

Figure 3. Finite element simulation of the effect of a sound bar partially covering a cylindrical tube

the bar. The sound radiated by the bars is amplified by Helmholtz resonators which are in the focus of the present study. When the resonators are designed, the effect of the sound bars partially covering the opening of the resonator needs to taken into consideration. In case of marimbas with quarter-wavelength tube resonators a practical guideline is to tune the natural frequency of the resonator about 3% sharp [7]. The detuning effect of sound bars is examined in the sequel. First, the effect of a single sound bar is considered, and the length correction due to the sound bar is predicted with varying the geometrical parameters of the arrangement. Then, an assembled instrument is investigated and the measured, simulated, and predicted natural frequencies of the resonators are evaluated and compared to each other.

### 4.1 The length correction effect of a sound bar

First, a single sound bar partially covering the circular opening of a resonator is studied by the FEM using a model geometry. Figure 3(a) shows the arrangement of the simulation. The cylindrical tube is driven by a plane wave with unit amplitude. The tube radiates into an open half-space, shown by the box-shaped region in the figure. As the length of the sound bars is much greater than the radius of the opening of the resonators, the bar is assumed to be infinitely long along the $y$ axis. The problem has two symmetry planes ($x = 0$ and $y = 0$ in our case), thus, only a quarter of the whole geometry is meshed. On the symmetry surfaces zero normal velocity boundary condition is applied. Infinite elements are attached to the free surfaces of the box-shaped region.

The main parameters that are varied are the width and the thickness of the bar $w$ and $t$, respectively, and the distance $h$ between the open end of the tube and the sound bar. These lengths are non-dimensionalized by the radius of the tube $r$. Simulations were performed under the cut-on frequency of the first transverse mode of the tube, i.e. $kr < 1.84$, and the radiation impedance and the length correction were extracted. A typical simulation result showing the asymmetric radiation pattern is displayed in Figure 3(b).

The freqeuncy dependent length correction coefficients $\Delta L/r$ are displayed in Figure 4. The length correction of an open tube in an infinite baffle without sound bar is plotted in each diagram with a dashed line as a reference. The thickness of the bar is found to have only a minor effect on the radiation impedance; and in the diagrams the case $t = 0.6r$ is shown. In the left diagram the effect of the width of bar is visible with $h = r$ kept constant. As seen, the presence of the bar increases the length correction at low freqeuncies in all cases and the effect becomes larger with increasing the width of the bar. Interestingly, until $w < 2r$ the length correction decreases monotonically with the frequency, while for $w > 2r$ the correction increases in the low frequency range and

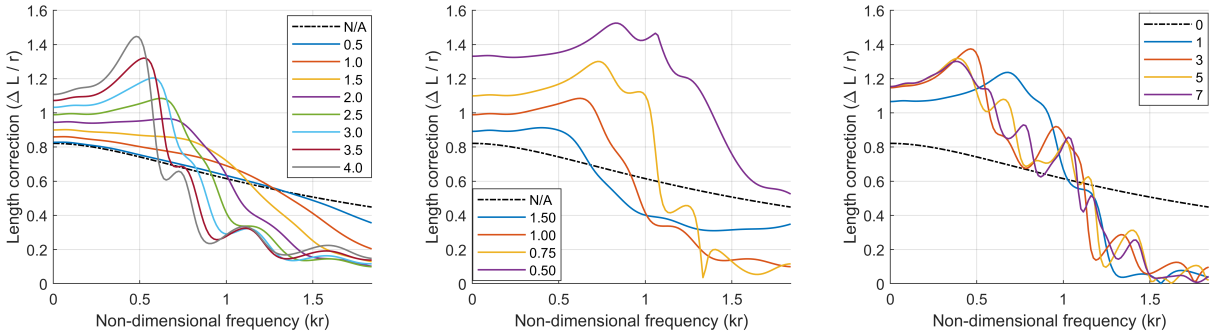


(a) Different widths $w/r$ (b) Different distances $h/r$ (c) Different number of bars $n$

Figure 4. Length correction effect of sound bars partially covering the open end of a cylindrical tube in different geometrical arrangements. The dash-dotted line shows the reference setup without sound bars.

decays quickly after reaching its maximum. The center digram shows the effect of changing the distance $h$ of the bar from the opening of the tube while keeping the width constant as $w = 2.5r$. As observed, the length correction is very sensitive to the distance, and increases with decreasing the distance $h$. In case of $h = 0.5r$ the low frequency correction effect is more than 60% greater than that without the bar.

Figure 4(c) shows the length correction effect taking a number of adjacent bars also into account. As the arrangement is symmetric (see Figure 3(a)) the number of sound bars is odd. The diagram shows the case with the parameters chosen as $h/r = 0.8$ and $w/r = 2.5$. The width of the gap between the bars is set as $g/r = 0.56$ which corresponds to the geometry studied in the next section. As seen, the effect of the adjacent bars on the length correction is significant. Adding the neighboring bars increases $\Delta L$ in the low frequency range by $\approx 8\%$, while the effect of adding further sound bars is negligible. At higher frequencies the length correction oscillates due to multiple reflections inside the gaps between the bars and the infinite baffle and the bars.

### 4.2 Examination of assembled resonators

The resonators of the assembled instrument were studied next, using measurements, finite element models, and predictions based on the length correction study presented in the previous section. The natural frequencies of the resonators are determined with and without sound bars and the detuning effect of the bars is quantified and compared with the results of the predictive model. Both in the measurements and simulations the resonators were driven using an external excitation signal. The excitation was provided by a loudspeaker in the measurements and modeled as an ideal point source in the simulations. The sound pressure response at one point inside the resonator was recorded and a transfer function was calculated by dividing the spectrum with that of the reference signal recorded close to the loudspeaker. The natural frequency is found as the maximum location of the transfer function and the quality factor is estimated using the 3 dB-width of the curve.

The natural resonance frequency $f_{\mathrm{hr}}$ of a Helmholtz resonator is expressed as

$$f_{\mathrm{hr}} = \frac{c}{2\pi}\sqrt{\frac{S}{V L_{\mathrm{eff}}}} \qquad \text{with} \qquad L_{\mathrm{eff}} = L + \Delta L_{\mathrm{in}} + \Delta L_{\mathrm{out}}, \tag{4}$$

where $S$ is the area of the opening, $V$ is the volume of the cavity, and $L_{\mathrm{eff}}$ is the effective length of the neck resulting as the sum of its physical length $L$, and the inner and outer corrections $\Delta L_{\mathrm{in}}$ and $\Delta L_{\mathrm{out}}$. When no sound bars are present, radiation into a half-space can be assumed with the corrections $\Delta L_{\mathrm{out}} = \Delta L_{\mathrm{in}} = 0.82r$. In case of the examined experimental instrument the physical length of the neck is very small, $L = 3\,\mathrm{mm}$ while the radius of the openings is $r = 12.5\,\mathrm{mm}$, and hence the effective length is dominated by the length corrections. Thus, the

| | | Without sound bars | | | | | With sound bars | | | | | Detuning | | | |
|---|---|---|---|---|---|---|---|---|---|---|---|---|---|---|---|
| | | Meas | FE | | Lossy FE | | Meas | FE | | Lossy FE | | Meas | FE | Predicted | |
| Note | Volume [cm$^3$] | $f$ [Hz] | $f$ [Hz] | $Q$ [–] | $f$ [Hz] | $Q$ [–] | $f$ [Hz] | $f$ [Hz] | $Q$ [–] | $f$ [Hz] | $Q$ [–] | $\Delta f$ [%] | $\Delta f$ [%] | $\Delta f$ [%] | $\Delta L/r$ [–] |
| #1 | 992.88 | 239 | 254 | 71 | 253 | 49 | 228 | 244 | 79 | 244 | 52 | −4.6 | −3.6 | −4.3 | 0.99 |
| #4 | 482.72 | 332 | 349 | 55 | 348 | 41 | 313 | 335 | 63 | 333 | 45 | −5.7 | −4.3 | −4.9 | 1.02 |
| #7 | 262.74 | 476 | 483 | 38 | 481 | 31 | 449 | 460 | 44 | 458 | 34 | −5.7 | −4.8 | −4.9 | 1.02 |
| #10 | 148.96 | 691 | 691 | 22 | 688 | 19 | 606 | 632 | 29 | 630 | 25 | −12.3 | −8.4 | −8.1 | 1.17 |
| #13 | 84.00 | 920 | 938 | 15 | 933 | 13 | 860 | 873 | 17 | 867 | 15 | −6.5 | −7.0 | −6.0 | 1.07 |

Table 1: Comparison of measured and calculated resonance properties of different resonators of a mallet percussion instrument. “Meas”: measurement, “FE”: finite element simulation, “Lossy FE”: FE with viscous losses, “Predicted”: prediction of detuning using the hybrid model.

frequency of natural resonance is sensitive to the length correction and a significant detuning can be expected due to the presence of sound bars. To be able to quantify the importance of viscous losses, the FE model was extended following [8] to account for viscothermal wall effects. The formulation specifies an equivalent wall admittance, which adds a diagonal component to the damping matrix $\mathbf{C}$ of (1). As the admittance depends on the angle of incidence which is not known a priori, the equation is solved in an iterative manner starting from lossless walls and updating the admittance in each step. Convergence is reached in a few iterations.

Table 1 compares the measurement, simulation, and prediction results for five of the thirteen resonators of the experimental instrument. It is noted that the data represents a raw state of the instrument, i.e., the resonators are not tuned precisely to musical pitch. A good agreement of the simulated and measured results are observed with the greatest deviation of the frequencies being $\approx 6\%$ in case of resonator #4. The geometry of the arrangement is fairly complex as the resonators have irregular shapes and the sound bars cover the openings to different extents. To preserve an equivalent spacing of the bars, the openings of the resonators are not at the center position but are slightly shifted towards the end of the bars. Due to the arch-shaped longitudinal section of the bars, this results in different distances of resonator openings and sound bars. Furthermore, resonators #1 and #13 are the first and last of the instrument and hence their neighboring sound bars are arranged asymmetrically.

The effect of viscothermal losses on the natural frequency is found to be small with the largest difference being $< 1\%$ in case of resonator #13. However, the quality factor is affected by the wall losses to a significant extent in case of the resonators with lower natural frequencies. This result is explained by the radiation losses being lower in the low frequency range. At higher frequencies the radiation losses become dominant and the effect of viscous losses is smaller. The quality factors were also evaluated from the measurements, however, the results exhibited a large amount of scatter and thus the values are not shown in the table. Nevertheless, predicting the expected quality factor of a resonator is useful as, beside the natural frequencies, the quality factors also need to be tuned. Too high quality factors result in an easy detuning from the vibration frequency of the sound bar by the change of the environmental temperature, for example, while a too low quality factors lead to unsatisfactory amplification of the radiated sound.

Finally, the detuning effect of the sound bars was examined. The last column of Table 1 shows the estimated length correction coefficient $\Delta L_{\text{out}}/r$ for the resonators taking the aforementioned geometrical differences of the sound bar arrangement into account. The natural frequencies are in the range $0.05 < kr < 0.25$, thus, a low frequency approximation of the length correction was used. The predictions are based on the parametric finite element study presented in Section 4.1. As seen, the predicted detuning is in very good agreement with the results of the full finite element model and these two models are also in good correspondence with the measurements. The greatest deviation of $\approx 4\%$ is observed in case of resonator #10, while the differences are $< 1\%$ in other cases. One possible cause of the deviations between the measured and modeled resonance

properties is the inevitable excitation of wall vibrations in the measurements. While the finite element models assume perfectly rigid walls, the relatively thin plastic walls of the resonators are easily excited by the external loudspeaker. It was already found that the sound bars must be damped when measuring the transfer function of the resonators; however, the inner walls could not be damped without changing the volume of the resonators. Despite the observed discrepancies, it can be assessed that the detuning effect is reproduced well by both the finite element and the hybrid models.

## 5 CONCLUSIONS

This paper examined two applications of a numerical approach [1] for calculating the radiation impedance of resonators having irregular geometries. In the first study sound radiation from the mouth of flue instruements was examined and the simulation results were compared with measurement data and models published previously. The simulated length correction effect of different recorders agreed well with the measurements and models of [3] and [5]. In case of a cylindrical organ pipe a minor modification of the model presented in [5] lead to a very good agreement with the simulations for all examined geometries. The second study investigated the design of the resonators of a mallet percussion instrument. The detuning effect of a sound bar was found to be significant, and it was also shown that the neighboring sound bars also have a non-negligible detuning effect. Making use of the length corrections determined in a simplified arrangement, the detuning of the resonators of the experimental instrument was predicted accurately. Both applications highlight the usefulness and versatility of the proposed impedance modeling approach.

## ACKNOWLEDGEMENTS

P. Rucz acknowledges the support of the Bolyai János research grant provided by the Hungarian Academy of Sciences. Supported by the ÚNKP-18-4 New National Excellence Program of the Ministry of Human Capacities.

## REFERENCES

[1] P. Rucz. A finite element approach for the calculation of self and mutual radiation impedances of resonators. *Journal of the Acoustical Society of America*, 143(4):2449–2459, 2018.

[2] F. Ingerslev and W. Frobenius. Some measurements of the end-corrections and acoustic spectra of cylindrical open flue organ pipes. *Transactions of the Danish Academy of Technical Sciences*, 1(3):1–42, 1947.

[3] D. H. Lyons. Resonance frequencies of the recorder (English flute). *Journal of the Acoustical Society of America*, 70(5):1239–1247, 1981.

[4] M. P. Verge, B. Fabre, W. E. A. Mahu, A. Hirschberg, R. R. van Hassel, A. P. J. Wijnands, J. J. de Vries, and C. J. Hogendoorn. Jet formation and jet velocity fluctuations in a flue organ pipe. *Journal of the Acoustical Society of America*, 95(2):1119–1132, 1994.

[5] A. Ernoult and B. Fabre. Window impedance of recorder-like instruments. *Acustica-Acta Acustica*, 103:106–116, 2017.

[6] C. Geuzaine and J.-F. Remacle. Gmsh: a three-dimensional finite element mesh generator with built-in pre- and post-processing facilities. *International Journal for Numerical Methods in Engineering*, 79(11):1309–1331, 2009.

[7] I. Bork. Practical tuning of xylophone bars and resonators. *Applied Acoustics*, 46:103–127, 1995.

[8] A. Lefebvre, G. P. Scavone, and J. Kergomard. External tonehole interactions in woodwind instruments. *Acustica-Acta Acustica*, 99:975–985, 2013.